Nonlinear collective oscillations of an ion cloud in a Paul trap

R. Alheit, X. Z. Chu,* M. Hoefer, M. Holzki, and G. Werth
Institut für Physik, Johannes-Gutenberg Universität, D-55099 Mainz, Germany

R. Blümel
Fakultät für Physik, Albert-Ludwigs Universität, D-79104 Freiburg, Germany

(Received 12 June 1997)

In an experiment using a Paul trap, we create a H_2^+ ion cloud by electron ionization of the background gas at 10^{-9}-mbar residual pressure. Exciting the ions parametrically at twice the frequency of the secular motion of ions in the r or z direction, we observe a narrow resonance at some distance from the motional resonance center if the amplitude of the exciting field exceeds a threshold value. The threshold value decreases with increasing ion number. Since the narrow resonance does not shift with ion number, we interpret it as a collective resonance of the center of mass of the ion cloud. The resonance shape exhibits the typical form of a driven anharmonic oscillator. The conclusions drawn from the experiments are supported by detailed analytical and numerical computations. [S1050-2947(97)05211-6]

PACS number(s): 32.80.Pj, 07.75.+h

I. INTRODUCTION

Over the past decade many authors have demonstrated, experimentally as well as theoretically, that the Paul trap [1,2] is an excellent microlaboratory for the investigation of nonlinear dynamics. Many effects, such as, e.g., rf heating [3], or the crystallization and melting of simultaneously stored charged particles [4], elusive for decades, have been interpreted and explained within the framework of nonlinear dynamics and chaos [5–7]. New nonlinear effects were predicted, both on the classical [8,9] and quantum levels [10]. The purpose of this paper is the explanation of another nonlinear effect with a long history: the excitation of collective motion of an ion cloud in a real Paul trap by an additional frequency. This effect was first described about 30 years ago by Rettinghaus, and correctly identified as a collective resonance [11]. It was also seen by Jungmann *et al.* [12] and by Vedel and co-workers [13,14]. The mechanism of this effect, however, remained elusive. As described in more detail below, we interpret the effect as a parametric resonance of the center-of-mass motion of the ion cloud [15,16]. Thus the central point of our paper is not the presentation of the collective resonance, which has been seen before, but a detailed analysis of the excitation mechanism supported by theoretical computations. We also present detailed investigations of the shape of the collective resonance, together with nonlinear effects that appear in the vicinity of the collective resonance.

It is clear that a real Paul trap, i.e., the actual device used in laboratory experiments, is never an ideal quadrupole. Due to the finiteness of the electrodes, deviations from axial symmetry, observation holes in the electrodes, etc., the field of a real Paul trap contains higher multipole components with appreciable strength. Thus even the center-of-mass motion of an ion cloud in a real Paul trap is highly nonlinear. Driven by an additional frequency, it is akin to the Duffing oscillator [17] which displays a cornucopia of nonlinear effects [17–19]. Thus, apart from elucidating the excitation mechanism of the collective resonance of an ion cloud in a real Paul trap, we also discuss briefly additional nonlinear effects expected to be observable in the center-of-mass motion of driven ion clouds in a real Paul trap. We present preliminary experimental evidence in support of our predictions. All our experimental results are backed by detailed numerical and analytical computations.

The paper is organized in the following way. In Sec. II we present a brief description of our experiment. In Sec. III we discuss the basic equations of motion of an ion cloud in the nonlinear potential of a real Paul trap. This section serves to set the stage and to introduce the notation needed for subsequent sections of the paper. In Sec. IV we present our experimental data on the existence of the collective resonance. In Sec. V we analyze the properties of the collective resonance on the basis of the equations of motion obtained in Sec. III. Many of the observed resonance characteristics hinge on the existence of a damping mechanism of the cloud motion. Since in the experiments reported in this paper we do not use any explicit cooling methods, such as, e.g., buffer gas or laser cooling [20], the nature of the damping mechanism in our experiments is as yet unclear. One candidate mechanism is damping of the cloud by the ambient rest gas. This mechanism and its consequences are presented in Sec. VI. In Sec. VII we discuss our results. In Sec. VIII we summarize and conclude the paper.

II. EXPERIMENTAL SETUP AND PROCEDURES

In the experiments reported in this paper we study the nonlinear response of H_2^+ ion clouds stored in a Paul trap to an additionally applied ac voltage referred to as the ''excitation voltage.'' We accomplish this aim by measuring the survival rate of H_2^+ ions in the presence of the excitation field for a well-defined excitation frequency, amplitude, and interaction time. We refer to this type of experiments as excitation experiments. A schematic sketch of our setup is

*Permanent address: Dept. of Electronics, Peking University, Beijing 100871, P. R. China.

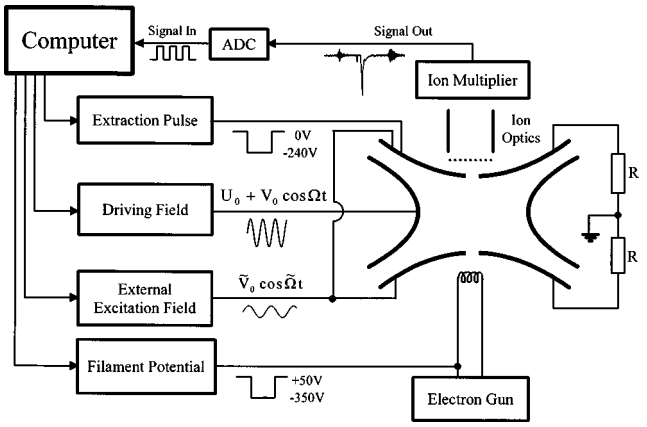

FIG. 1. The experimental setup.

shown in Fig. 1. Apart from the dimensions of the Paul trap, it has already been described in detail in Refs. [21, 22]. Thus we restrict ourselves here to a presentation of only those experimental features that are essential for the discussion below.

The core of our experiment is a Paul trap consisting of a hyperbolic ring electrode with an inner radius of $r_0 = 2$ cm and two hyperbolic end caps whose distance of closest approach is $2z_0 = \sqrt{2} r_0$. The trap is operated at a frequency of $\Omega/2\pi = 3$ MHz. A typical excitation experiment consists of three stages.

(i) Creation stage. In this stage, of temporal duration T_c, the H_2^+ ions are created inside the trap by electron bombardment of the rest gas which is held at 10^{-9} mbar. We refer to T_c as the creation time. It is typically of the order of 1 s.

(ii) Interaction stage. After creating the H_2^+ ions, they are exposed to a superposition of the trap fields and the excitation field during a time T_i, referred to as the interaction time. The interaction time T_i can be changed experimentally from a few ms to arbitrarily long times. In practice, however, an upper limit of T_i is given by the ion storage time which is typically of the order of 8–10 s under our experimental conditions. During the interaction stage both end caps of the trap are electrically connected. This observation is important, since it rules out dipole excitation of the ion clouds.

(iii) Detection stage. Following the interaction stage, we extract the ions with the help of a field pulse through the upper end cap of the trap. The extraction pulse is phase correlated with the trap's ac driving field. The ions arrive at the first dynode of a multiplier tube and create an electron pulse whose total charge is proportional to the ion number. The pulse is amplified and digitized and fed to a personal computer for further data handling. Different mass ions arrive at the detector at different times. H_2^+ ions are selected by setting an amplifier gate at proper timing. The total detection efficiency, including ion loss in the time-of-flight region and quantum efficiency of the multiplier, is estimated to be 10%.

A motional resonance is detected by a decrease of the ion number arriving at the detector. We should emphasize that for every data point in our experimental observation, the ions are lost from the trap, and new ions have to be created for the next point. Thus the ions under investigation do not have a ''memory'' concerning previous excitations. This is of importance for the shape of the observed resonances.

III. MICROSCOPIC DESCRIPTION

In this section we establish the notation used in subsequent sections, and present the classical equations of motion of an ion cloud in the dynamic potential of a real Paul trap. The classical point of view is sufficient for our purposes, since the kinetic energy of the ions in our experiments is very large: we estimate the temperature of the ion cloud to be of the order of a thousand Kelvin. Thus quantum effects are negligible.

The multipole expansion of the potential of a real Paul trap is given by

$$\Phi(\vec{r}) = -V(t) \sum_{k=1}^{\infty} C_k \left(\frac{r}{r_0} \right)^k P_k(\cos\,\theta), \tag{1}$$

where

$$V(t) = U_0 + V_0 \cos(\Omega t) + \tilde{V}_0 \cos(\tilde{\Omega} t). \tag{2}$$

The constants C_k in Eq. (1) are the strengths of the multipole components of the trap, r_0 is the radius of the ring electrode, and the functions P_k are the Legendre Polynomials as defined, e.g., in Ref. [23]. In our analytical and numerical computations to be discussed below, we include multipole components up to $k = 4$ (octopole). The constants U_0 and V_0 in Eq. (2) are the dc and ac trap voltages, and $\tilde{V}_0$ is the excitation voltage. The trap frequency and the excitation frequency are denoted by Ω and $\tilde{\Omega}$, respectively. Using r_0 as the unit of length, we obtain the following equations of motion for N ions in the trap:

$$\begin{aligned}
&\frac{d^2}{d\tau^2} \begin{pmatrix} x_i \\ y_i \\ z_i \end{pmatrix} + \gamma \frac{d}{d\tau} \begin{pmatrix} x_i \\ y_i \\ z_i \end{pmatrix} \\
&\quad = [a + 2q\,\cos(2\tau) + 2\tilde{q}\,\cos(\omega\tau + \varphi)] \\
&\qquad \times \left\{ C_1 \begin{pmatrix} 0 \\ 0 \\ 1 \end{pmatrix} + 2C_2 \begin{pmatrix} -x_i/2 \\ -y_i/2 \\ z_i \end{pmatrix} + 3C_3 \begin{pmatrix} -x_i z_i \\ -y_i z_i \\ z_i^2 - \rho_i^2/2 \end{pmatrix} \right. \\
&\qquad \left. + 4C_4 \begin{pmatrix} 3x_i\rho_i^2/8 - 3x_i z_i^2/2 \\ 3y_i\rho_i^2/8 - 3y_i z_i^2/2 \\ z_i^3 - 3z_i\rho_i^2/2 \end{pmatrix} \right\} + \alpha \sum_{\substack{j=1 \\ j \neq i}}^{N} \frac{\vec{r}_i - \vec{r}_j}{|\vec{r}_i - \vec{r}_j|^3}, \\
&\qquad\qquad i = 1, \ldots, N.
\end{aligned} \tag{3}$$

In Eq. (3) the position of ion number i is defined as $\vec{r}_i = (x_i, y_i, z_i)$; $a \equiv a_r$ and $q \equiv q_r$ are the conventional Paul trap control parameters given by

$$a = \frac{4QeU_0}{m\Omega^2 r_0^2}, \quad q = \frac{2QeV_0}{m\Omega^2 r_0^2}, \tag{4}$$

where m and Q are the mass and the charge number of the trapped particles, τ is the dimensionless time

$$\tau = \Omega t/2; \tag{5}$$

$\omega = 2\tilde{\Omega}/\Omega$ is the dimensionless excitation frequency, $\rho^2 = x^2 + y^2$; and α is the strength of the Coulomb potential, in our units given by

$$\alpha = \frac{Q^2 e^2}{m\Omega^2 \pi \epsilon_0 r_0^3}. \tag{6}$$

The control parameter $\tilde{q}$ is the dimensionless strength of the additionally applied excitation voltage. It is related to the control parameter q by $\tilde{q} = q\tilde{V}_0/V_0$. The relative phase between the trap voltage and the excitation voltage is denoted by φ in Eq. (3). The generators of the trap voltage and the excitation voltage are not phase locked. Thus in our current experiments φ is unknown, but does not affect the results of our experiments. Thus we will set $\varphi = 0$ in the following discussion.

For $\tilde{q} = 0$, neglecting the nonlinear terms in Eq. (3) and assuming a perfect axial symmetry, the dimensionless secular frequencies in the x, y, and z directions are given by

$$\omega_r \equiv \omega_x = \omega_y \approx \sqrt{a + q^2/2}, \quad \omega_z \approx \sqrt{2(q^2 - a)} \tag{7}$$

for small a and q. We added a damping term to Eq. (3) with a damping constant γ. Within the framework of our derivations this damping term has no microscopic justification. But damping is certainly present experimentally. Possible damping mechanisms include collisions with rest gas atoms, energy dissipation by polarization charges in the trap electrodes, or irreversible deformations of the ion cloud caused by the oscillation of the cloud in the anharmonic potential of the trap. The set of equations (3) is the basis for the theoretical analysis of the experimental results reported in this paper. Set (3) is used in two different ways. (i) directly as the basis for our microscopic three-dimensional numerical simulations and (ii) as the starting point for an analytical investigation of the cloud motion. We will see in Sec. V below that the analytical results derived from Eq. (3) reproduce the results obtained from full-fledged numerical three-dimensional simulations of Eq. (3) to an astonishing degree of accuracy.

IV. COLLECTIVE RESONANCE

In this section we present experimental and numerical evidence of the existence of a sharp collective resonance at an excitation frequency $\omega \approx 2\omega_z$. We observe a similar phenomenon at $\omega \approx 2\omega_r$ [24]. The shape of the $\omega \approx 2\omega_r$ resonance is qualitatively the same as the shape of the $\omega \approx 2\omega_z$ resonance. In this paper we restrict ourselves to the discussion of the $2\omega_z$ resonance.

The central result of our experiments with an additionally applied excitation frequency is shown in Fig. 2. Plotted is the number of detected ions as a function of the excitation frequency for five different excitation voltages. We see a broad resonance at $\omega \approx 2\omega_z$. We call this resonance the ''mother resonance.'' Figure 2 shows that we also observe an additional narrow resonance which appears at the high-frequency wing of the mother resonance if the excitation amplitude exceeds a certain threshold value. We call this resonance the ''daughter resonance.''

The nature of the mother and daughter resonances is best illuminated by investigating the space-charge dependence of

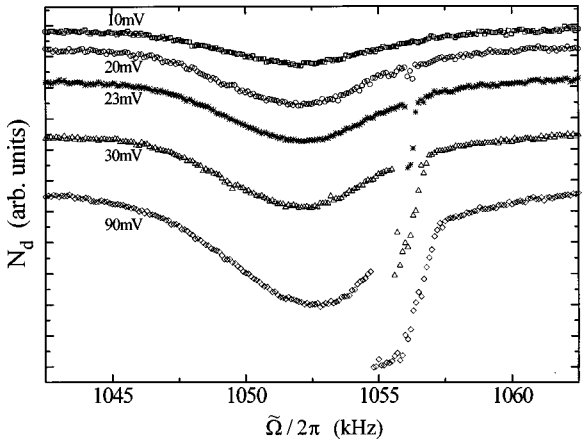

FIG. 2. Number of detected ions N_d for mother and daughter resonances as a function of excitation frequency $\tilde{\Omega}/2\pi$ for five different excitation voltages. The initial number of ions for the five different curves are the same. We shifted these curves vertically for clarity of presentation.

the two resonances. Figure 3 shows the frequency locations $\Omega_c/2\pi$ (the central frequencies) of the two resonances as a function of the number of detected ions. While the location of the mother resonance shifts with ion number, the location of the daughter resonance is constant and thus space-charge independent. On the basis of this observation we interpret the mother resonance as due to resonant but incoherent rf heating of the ion cloud, and the daughter resonance as due to a collective oscillation of the ion cloud as a whole, i.e., as an excitation of the center-of-mass coordinate of the ion cloud. This interpretation is consistent with the one found in the literature [11–14].

We support the interpretation of the daughter resonance as a collective oscillation of the center of mass of the ion cloud by a direct numerical simulation of the equations of motion (3). We use a fourth-order Runge-Kutta method to integrate the set of equations (3) for a random initial condition of the ions in the cloud for ten ions. The random initial condition simulates the stochastic creation process of the ions in our experiment. We define the center of mass of the ion cloud

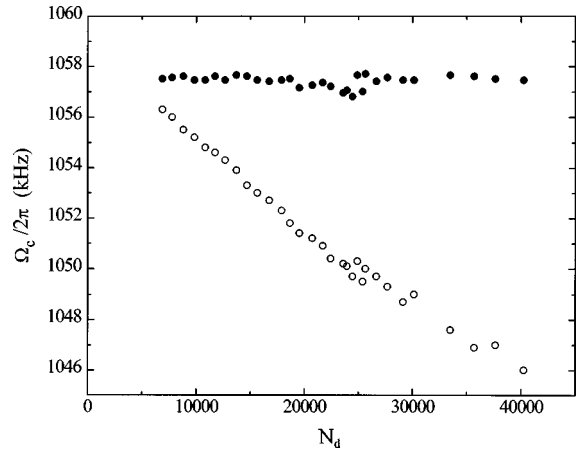

FIG. 3. Central frequencies $\Omega_c/2\pi$ of mother and daughter resonances as a function of the number of detected ions N_d. Open circles: mother resonance. Solid circles: daughter resonance.

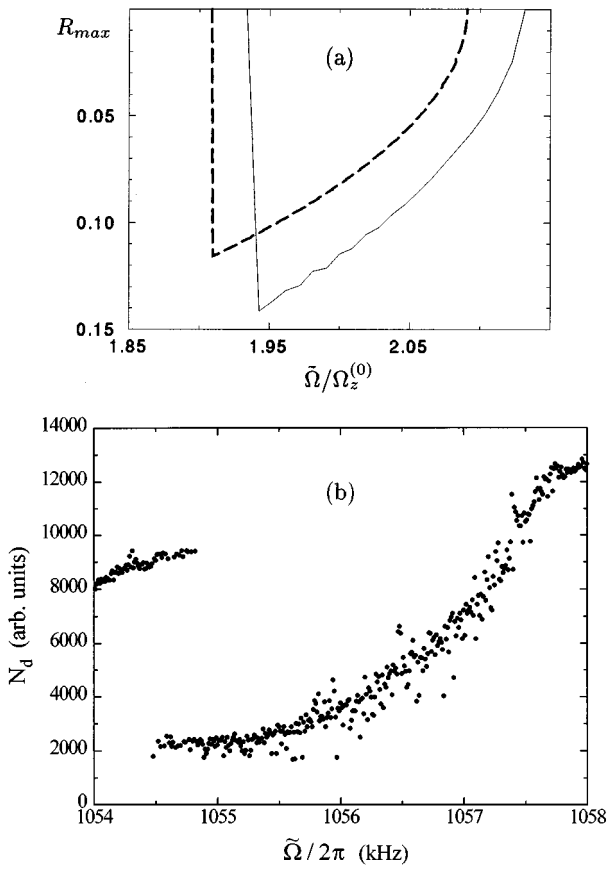

FIG. 4. The shape of the collective resonance. (a) Theoretical results. The maximal excursion amplitude $R_{\max}$ as a function of the scaled excitation frequency $\tilde{\Omega}/\Omega_z^{(0)}$, where $\Omega_z^{(0)}=\Omega\omega_z/2$ is the ''unperturbed'' secular frequency of the trap according to Eq. (7). The potential parameters and the damping constant are chosen according to Eq. (21). Full line: $R_{\max}$ obtained from three-dimensional computer simulations of the equations of motion (3). Dashed line: analytical result (34) derived from the one-dimensional model of Z motion. (b) Experimental results. Shown is the number of detected ions N_d as a function of the excitation frequency $\tilde{\Omega}/2\pi$. The experimental result shows bistability of the trapped ion cloud in the vicinity of the transition between mother resonance and collective resonance.

$$\vec{R}\equiv\begin{pmatrix}X\\Y\\Z\end{pmatrix}=\frac{1}{N}\sum_{i=1}^{N}\begin{pmatrix}x_i\\y_i\\z_i\end{pmatrix}, \tag{8}$$

and the relative coordinates

$$\begin{pmatrix}\xi_i\\\eta_i\\\zeta_i\end{pmatrix}\equiv\vec{r}_i-\vec{R}. \tag{9}$$

We also define $R_{\max}(\omega)$ as the maximal excursion of $|\vec{R}|$ at a fixed excitation frequency ω. The full line in Fig. 4(a) shows $R_{\max}$ obtained as a result of our ten-ion simulations. For easier comparison with the experimental result shown in Fig. 4(b), $R_{\max}$ is drawn in the negative y direction. We see that $R_{\max}$ is different from zero only in a narrow frequency interval which corresponds to the collective resonance. Moreover, $R_{\max}$ is of appreciable magnitude, which explains the large ion loss in the vicinity of the collective resonance.

Using reasonable assumptions, our aim now is to derive the equations of motion for $\vec{R}$ in the vicinity of $\omega=2\omega_z$. We assume that for $\omega\approx2\omega_z$ only the z component of $\vec{R}$ is excited, i.e., $X=Y=0$. This assumption is confirmed by our numerical simulations of the full set of equations (3). Thus, the physics of the cloud motion at $\omega\approx2\omega_z$ is contained in the z degree of freedom of the cloud and we concentrate on deriving an equation of motion for Z. Because of

$$\sum_{i=1}^{N}\sum_{\substack{j=1\\j\neq i}}^{N}\frac{\vec{r}_i-\vec{r}_j}{|\vec{r}_i-\vec{r}_j|^3}=0, \tag{10}$$

the Coulomb term in Eq. (3) drops out of the equation of motion for Z, and we obtain

$$\ddot{Z}+\gamma\dot{Z}=[a+2q\,\cos(2\tau)+2\tilde{q}\,\cos(\omega\tau)][C_1+2C_2Z+3C_3\langle z^2\rangle-3C_3\langle\rho^2\rangle/2+4C_4\langle z^3\rangle-6C_4\langle\rho^2 z\rangle], \tag{11}$$

where we used the notation

$$\langle z^\nu\rho^\mu\rangle=\frac{1}{N}\sum_{i=1}^{N}z_i^\nu\rho_i^\mu. \tag{12}$$

Defining

$$r_\rho^2\equiv\langle\rho^2\rangle=\frac{1}{N}\sum_{i=1}^{N}(\xi_i^2+\eta_i^2),\quad r_z^2=\frac{1}{N}\sum_{i=1}^{N}\zeta_i^2 \tag{13}$$

and assuming that the ion cloud is symmetric enough such that

$$\sum_{i=1}^{N}\zeta_i^3\approx0, \tag{14}$$

we obtain

$$\langle z^2\rangle=Z^2+r_z^2,\quad\langle\rho^2\rangle=r_\rho^2,\qquad\langle z^3\rangle=Z^3+3Zr_z^2. \tag{15}$$

For the computation of $\langle\rho^2 z\rangle$, we assume, additionally, the independence of the relative motion of the ions in the cloud in ρ and z directions, i.e.,

$$\langle\rho^2 z\rangle=\langle\rho^2\rangle\langle z\rangle=Zr_\rho^2. \tag{16}$$

Inserting Eqs. (15) and (16) into Eq. (11), we obtain

$$\ddot{Z}+\gamma\dot{Z}=[a+2q\,\cos(2\tau)+2\tilde{q}\,\cos(\omega\tau)]\sum_{\nu=0}^{3}f_\nu Z^\nu, \tag{17}$$

where

$$f_0=C_1+3C_3(r_z^2-r_\rho^2/2),\quad f_1=2C_2+12C_4(r_z^2-r_\rho^2/2),\qquad f_2=3C_3,\quad f_3=4C_4. \tag{18}$$

In order to obtain some analytical insight into the solutions of Eq. (17) in the vicinity of $\omega \approx 2\omega_z$, we observe that for the conditions of the experiment $\omega \approx 2\omega_z \ll 2$. Thus, with respect to the excitation frequency ω, the term proportional to q in Eq. (17) is rapidly oscillating and can be replaced by a time-independent pseudopotential [3,25]. We obtain

$$\ddot{Z} + \gamma \dot{Z} + \sum_{\mu=0}^{3} g_\mu Z^\mu = 2\tilde{q} \cos(\omega\tau) \sum_{\nu=0}^{3} f_\nu Z^\nu, \qquad (19)$$

where

$$g_0 = f_0[q^2 f_1/2 - a], \quad g_1 = q^2[f_1^2 + 2 f_0 f_2]/2 - a f_1,$$
$$g_2 = 3q^2[f_0 f_3 + f_1 f_2]/2 - a f_2, \quad g_3 = q^2[f_2^2 + 2 f_1 f_3] - a f_3. \qquad (20)$$

The structure of Eq. (19) is one of a driven, damped nonlinear oscillator. With Eq. (19), we are able to reproduce qualitatively the most prominent features of the experiments with the help of the following ''minimal model'' defined by

$$C_1 = 0, \quad C_2 = 1, \quad C_3 = 1, \quad C_4 = 0,$$
$$a = 0, \quad \gamma = 0.01, \quad r_z = r_\rho/\sqrt{2}. \qquad (21)$$

The parameters in Eqs. (21) are chosen according to the following considerations. As mentioned in Sec. II, the end caps of the trap are electrically connected during the interaction stage of an excitation experiment. Thus no dipole excitation is possible in z direction, and thus $C_1 = 0$. We choose $C_2 = 1$, since this is the correct strength for an ideal Paul trap. The hexapole component is chosen relatively large ($C_3 = 1$) in order to emphasize nonlinear effects. For the phenomena discussed in this paper the octopole term is not expected to produce qualitatively new effects and is set to zero. With choice of Eqs. (21) of model parameters the model equations are now given by

$$\ddot{Z} + \gamma \dot{Z} + \omega_z^2[Z + 9Z^2/2 + 9Z^3/2] = 2\tilde{q}[2Z + 3Z^2]\cos(\omega\tau), \qquad (22)$$

where, according to Eq. (7),

$$\omega_z = \sqrt{2} q. \qquad (23)$$

Let us now consider only the linear terms in Eq. (22), and, for the time being, put $\gamma = 0$. We obtain

$$\ddot{Z} + \omega_z^2 \left[1 - \frac{4\tilde{q}}{\omega_z^2} \cos(\omega\tau) \right] Z = 0. \qquad (24)$$

We substitute

$$\omega\tau = 2\hat{\tau}, \qquad (25)$$

and obtain

$$\ddot{Z} + \left(\frac{2\omega_z}{\omega} \right)^2 \left[1 - \frac{4\tilde{q}}{\omega_z^2} \cos(2\hat{\tau}) \right] Z = 0. \qquad (26)$$

This is an ordinary Mathieu equation of the form

$$\ddot{Z} + [\hat{a} - 2\hat{q} \cos(2\hat{\tau})] Z = 0, \qquad (27)$$

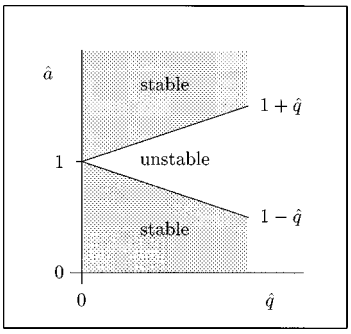

FIG. 5. Sketch of the stability diagram of the Mathieu equation with control parameters $\hat{a}$ and $\hat{q}$ in the vicinity of $\hat{a} \approx 1$ and $\hat{q} \approx 0$.

where

$$\hat{a} = (2\omega_z/\omega)^2, \quad \hat{q} = 8\tilde{q}/\omega^2. \qquad (28)$$

Since the Mathieu equation is known to exhibit parametric instabilities for small $\hat{q}$ at $\hat{a} = n^2$, $n = 1,2,\ldots$, we expect parametric instabilities of Eq. (26) at $\omega_n = 2\omega_z/n$. Of importance for our present experiments is the parametric instability for $n = 1$. We compute its width $\Delta\omega$ by following Ref. [25]. We define

$$\omega = 2\omega_z + \epsilon, \qquad (29)$$

where ϵ is small, and obtain

$$\ddot{Z} + \frac{1}{\left(1 + \frac{\epsilon}{2\omega_z}\right)^2} \left[1 - 2\left(\frac{2\tilde{q}}{\omega_z^2} \right) \cos(2\hat{\tau}) \right] Z = 0, \qquad (30)$$

where $\hat{a} \approx 1$, because ϵ is small. The stability diagram of Eq. (27) in the vicinity of $\hat{a} \approx 1$ is sketched in Fig. 5. According to Fig. 5 and up to linear order in $\hat{q}$, the solutions of Eq. (27) are unstable for $1 - \hat{q} < \hat{a} < 1 + \hat{q}$. Expanding Eq. (30) to leading order in ϵ, we obtain the instability of Eq. (30) for $|\epsilon| < 2\tilde{q}/\omega_z$. Thus, for negligible γ, the frequency width of the unstable region is

$$\Delta\omega = 4\tilde{q}/\omega_z. \qquad (31)$$

Including the damping, the width (31) is modified and given by [25]

$$\Delta\omega = \sqrt{(4\tilde{q}/\omega_z)^2 - (2\gamma)^2}. \qquad (32)$$

Thus we have isolated the physical origin of the collective resonance. It is revealed as a parametric instability of the driven nonlinear oscillator associated with the center-of-mass motion of the stored ion cloud. The model of the driven nonlinear oscillator also underlies the explanation of all other properties of the collective resonance, to be discussed in Sec. V.

V. PROPERTIES OF THE COLLECTIVE RESONANCE

Having established the existence of collective resonance in Sec. IV, we turn now to a more in-depth investigation of the properties of the collective resonance.

A. Strength of the resonance

Since the resonance corresponds to the instability region of a Mathieu equation, the trapped ions in this region are exponentially unstable, explaining the immediate onset of depletion of the trap in the instability region. Total depletion is stopped only because of the nonlinear terms in the trap potential.

B. Smallness of the drive

With the help of Eq. (31) we are now in a position to understand why a few mV of excitation voltage is enough to produce an appreciable width of the collective resonance. We write Eq. (31) in the form

$$\tilde{V}_0 = V_0 \tilde{q}/q \approx \left(\frac{\Delta\omega}{\omega_z}\right) q V_0/2. \tag{33}$$

Experimentally $\Delta\omega/\omega_z$ is of the order of 2.5×10^{-3}. Thus, at $q\approx0.15$, we have $\tilde{V}_0 \sim 2\times10^{-4} V_0$. Thus, if V_0 is of the order of several hundred V, $\tilde{V}_0$ is of the order of several tens of mV, which is consistent with the experimentally observed range.

C. Existence of a critical voltage

In all our experiments we observe that the collective resonance appears only for $\tilde{V}_0 > \tilde{V}_0^{(\mathrm{cr})}$. We call $\tilde{V}_0^{(\mathrm{cr})}$ the critical voltage. In our experiments the critical voltage is of the order of $\tilde{V}_0^{(\mathrm{cr})} \approx 15$ mV. As seen from Eq. (32), the existence of a critical voltage requires a finite damping constant γ. The critical excitation amplitude is then given by $\tilde{q}^{(\mathrm{cr})} = \gamma\omega_z/2$.

D. Shape of the resonance

Another feature of the collective resonance, which is explained by the simple model (22) is the shape of the collective resonance. Neglecting the nonlinear terms in the drive-term in Eq. (22), the oscillation amplitude $R_{\max}$ of Eq. (22) in the range $\Delta\omega$ of Eq. (30) is given by [25]

$$R_{\max} = \left\{ \frac{1}{\kappa} \left[\frac{\epsilon}{2} - \sqrt{\tilde{q}^2/\omega_z^2 - \gamma^2/4} \right] \right\}^{1/2}, \tag{34}$$

where the nonlinearity parameter κ of our model is given by [25]

$$\kappa = -\frac{27}{4}\omega_z. \tag{35}$$

The amplitude $R_{\max}$ is zero outside of $\Delta\omega$. Amplitude (34) is shown as the dashed line in Fig. 4(a). It is instructive to note that $R_{\max}$ obtained from the ten-ion simulations is shifted in frequency with respect to $R_{\max}$ computed according to Eq. (34). This is easily explained, since we calibrated the frequency axis in units of the ''unperturbed'' approximate frequencies (7). Thus the shift is due to the presence of nonlinear terms in the simulation calculations. Additional nonlinear terms not contained in κ (for instance, due to the Coulomb interaction), are responsible for the mismatch of the amplitudes between the simulations and Eq. (34).

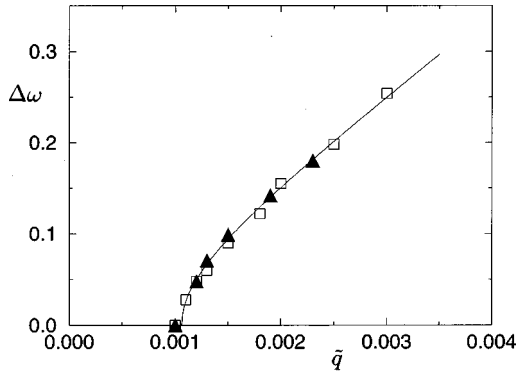

FIG. 6. Theoretical frequency width $\Delta\omega$ of the collective resonance. Full line: Analytical result (32). Squares: Frequency widths extracted from numerical solutions of Eq. (17). Triangles: Frequency widths extracted from three-dimensional numerical simulations of Eq. (3).

The shapes of the collective resonances shown in Figs. 4(a) and in 4(b) are qualitatively the same. Both show the kink at the high frequency end of the resonance and the steep cliff at the low frequency end. Details are different since $R_{\max}$ is not simply related to the ion loss in the trap. In order to compute the ion loss from $R_{\max}$, the Gaussian shape of the ion cloud [26] has to be taken into account.

E. Width of the resonance

In order to prove the validity of the approximations that led us to the pseudopotential form (22) of the minimal model, we computed the width $\Delta\omega$ by numerically solving the equations of motion (17), and in addition by solving the three-dimensional set of coupled equations (3) for ten H_2^+ ions. The result is shown in Fig. 6. The full line is the analytical result (32). The squares in Fig. 6 are the resonance widths obtained from the numerical solution of Eq. (17) and the triangles are the resonance widths computed from three-dimensional simulations of Eq. (3). There is no significant difference between all three results. This proves that the physical mechanism was correctly extracted from Eq. (3) and distilled into the simple driven oscillator (22). As a result of the theoretical analysis of Eq. (3), we are confident that the interpretation of the ''daughter resonance'' as a collective parametric resonance of the center of mass of the ion cloud is correct.

The theoretical results can be compared with experimental data. Figure 7 shows the frequency width $\Delta\Omega/2\pi$ of the collective resonance as a function of the excitation voltage. Figure 7 confirms the existence of a critical voltage, since the width of the collective resonance is zero for $\tilde{V}_0 < \tilde{V}_0^{(\mathrm{cr})} \approx 10$ mV. Moreover, the experimental width shows the typical nonanalytic behavior of a root singularity close to the critical voltage. The details of the experimental results, however, are not correctly reproduced by the simple analytical model. For instance, the experimental width shows a steep rise at high excitation voltage. The origin of this phenomenon is currently not understood.

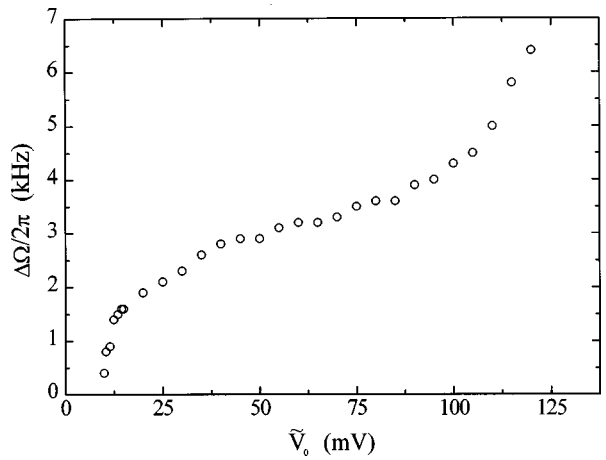

FIG. 7. Experimental frequency width $\Delta\Omega/2\pi$ of the collective resonance as a function of the excitation voltage $\tilde{V}_0$. The working points are $U_0=-5.0$ V, $V_0^{pp}=731$ V, and $\Omega/2\pi=3$ MHz ($a_z=0.0136$ and $q_z=0.4971$).

F. Bistability

One possible reason for the deviations of the analytical prediction for $\Delta\omega$ and the experimental results is the fact that the collective resonance exhibits bistability at its left-hand wing, i.e., at the sharp cliff where the collective resonance breaks and rejoins the mother resonance, as shown in Fig. 4(b). The bistability in the jump region is clearly visible. The existence of the bistability makes the determination of the width of the collective resonance somewhat ambiguous. This may account, at least partially, for the deviations between theory and experiment.

On the other hand, the existence of bistability is also a feature of the driven oscillator (22) [25]. Thus, as far as the mere existence of bistability of the collective resonance is concerned, theory and experiment are in agreement.

G. Critical voltage vs ion number

Another puzzling experimental result is the dependence of the critical voltage on the number of detected ions. We obtain

$$\tilde{V}_0^{(\mathrm{cr})}\sim 1/N^{1/3}. \tag{36}$$

This result is clearly borne out by the experimental data presented in the form of a log-log plot in Fig. 8. On the basis of our current understanding, the existence of a critical voltage requires the presence of a damping mechanism. Since no explicit damping methods are used in our experiments, the damping of the ion cloud occurs indirectly according to a mechanism which we have not yet properly identified, and cannot, at present, control. But whatever the damping mechanism, it must explain the observed $1/N^{1/3}$ behavior of the critical voltage. In Sec. VI, we offer a possible mechanism which indeed reproduces the $1/N^{1/3}$ law. We call this damping mechanism a ''candidate,'' since presently we see no possibility, neither experimental nor theoretical, of either confirming or rejecting this mechanism.

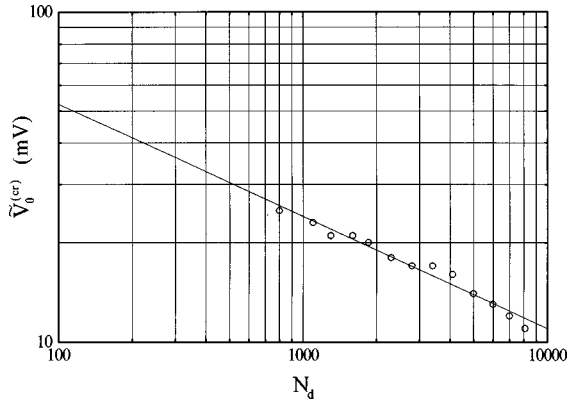

FIG. 8. Critical voltage $\tilde{V}_0^{(\mathrm{cr})}$ as a function of the number of detected ions N_d. The symbols are the experimental data points. The straight line is a least-squares fit assuming $\log_{10}(\tilde{V}_0^{(\mathrm{cr})})=A+B\log_{10}(N_d)$. We obtain $A=2.399\pm0.059$ and $B=-0.339\pm0.017$. The fit result indicates a relationship between the critical voltage $\tilde{V}_0^{(\mathrm{cr})}$ and the number N of ions in the cloud according to $\tilde{V}_0^{(\mathrm{cr})}\sim N^{-1/3}$.

VI. A CANDIDATE DAMPING MECHANISM

According to Eq. (32), the critical voltage is directly proportional to the damping constant, and is given by

$$\tilde{V}_0^{(\mathrm{cr})}=\frac{V_0\omega_z}{2q}\gamma. \tag{37}$$

One possible damping mechanism is the collision of the ion cloud with the molecules of the rest gas. Since the cloud moves in the z direction only, we represent it by a cross-sectional area A orthogonal to the z axis of the trap. The total mass of the cloud is denoted by M, its velocity by V. We now estimate the damping constant of the cloud on the basis of a simple gas-kinetic model. The density of the gas molecules of the rest gas is denoted by n, their mass by m and their rms velocity by v. For simplicity of the argument we assume that exactly 1/6 of the molecules fly in the positive z direction, and 1/6 fly in the negative z direction. The area A is struck by the gas molecules flying in positive z direction at a rate $(v-V)An/6$. The momentum transfer per impact is $\beta m(v-V)$, where β varies between 1 and 2 according to whether the molecule is absorbed by A or reflected off A. In the same way we find $(v+V)An/6$ and $-\beta m(v+V)$ for the rate of impact on A and the momentum transfer for gas molecules flying in negative z direction. Altogether, the force exerted by the gas molecules on the moving cloud becomes

$$F=-\frac{2\beta}{3}nAmvV. \tag{38}$$

Inserting Eq. (38) into the equation of motion for the center of mass of the ion cloud, we obtain

$$\frac{dV}{dt}=-\Gamma V, \tag{39}$$

where

$$\Gamma = \frac{2\beta A}{3M} nmv \tag{40}$$

may be interpreted as the damping constant of the ion cloud. Since $A \sim N^{2/3}$ and $M \sim N$, we obtain

$$\tilde{V}_0^{(\mathrm{cr})} \sim \Gamma \sim 1/N^{1/3}, \tag{41}$$

as measured in the experiment. The dimensionless damping constant γ used in Sec. III–V is related to Γ by

$$\gamma = \frac{2\Gamma}{\Omega} = \frac{4\beta A}{3M\Omega} nmv. \tag{42}$$

The expression for γ can be simplified. We use the usual gas-kinetic relations $p = mnv^2/3$ and $v^2 = 3kT/m$ to relate the density of the rest gas to the pressure, and the velocity to the temperature. Introducing an effective cross section such that

$$A = \sigma N^{2/3}, \tag{43}$$

we obtain

$$\gamma = \frac{2\beta\sigma p}{\Omega N^{1/3} v m_p}, \tag{44}$$

where m_p is the proton mass. For $\beta = 2$, $V_0 = 100$ V, and $p = 10^{-9}$ mbar, we observe experimentally a critical voltage of $\tilde{V}_0^{(\mathrm{cr})} \sim 20$ mV. This results in

$$\gamma \sim 10^{-4}. \tag{45}$$

Assuming $v \approx 1000$ m/s, $N \sim 10^6$, and $\Omega = 2\pi \times 3 \times 10^6$/s, we obtain the following estimate for σ:

$$\sigma \sim (1\ \mu\mathrm{m})^2. \tag{46}$$

This is not an unreasonable value. Thus the damping of the collective motion by the ambient rest gas is a possible damping mechanism.

VII. DISCUSSION

While there is little doubt about the nature and the existence of the collective resonance, its features leave considerable room for discussion. Currently the most puzzling experimental result is the existence of the critical voltage, and the detailed behavior of the width of the collective resonance as a function of the excitation voltage. As far as the critical voltage is concerned, we currently have no other explanation but to attribute it to damping of the motion of the ion cloud. A candidate mechanism, cooling by the ambient rest gas, was presented in Sec. VI. Although the main prediction of this mechanism, $\tilde{V}_0^{(\mathrm{cr})} \sim N^{-1/3}$ agrees with experiment, we are currently not able to test this mechanism in more detail in order to verify or discard it as the reason for the existence of the critical voltage $\tilde{V}_0^{(\mathrm{cr})}$. According to Eq. (44), $\gamma \sim p$ and, thus, $\tilde{V}_0^{(\mathrm{cr})} \sim p$. Thus one possible test of this mechanism is to measure $\tilde{V}_0^{(\mathrm{cr})}$ as a function of the pressure of the rest gas. This is not feasible with the present experimental setup, since we observe a rapid loss of H_2^+ ions from the trap at increasing background pressures, either by the reaction $H_2^+ + H_2 \rightarrow H_3^+ + H$ or by elastic collisions of H_2^+ with heavy background gas molecules.

Several other sources of damping exist. For instance, Ohmic dissipation of energy by induced charges in the electrodes of the trap. Another mechanism is ''internal dissipation'' of energy by deformation of the cloud due to the nonlinearities of the trap potential. This mechanism should be particularly effective at the turning points of the cloud. The effectiveness of this mechanism relies on the possibility of the cloud to absorb large amounts of energy. We do not have reliable expressions for the heat capacity of the cloud and are therefore currently not able to estimate the effectiveness of this mechanism.

The deviations of the width of the collective resonance from the expected square-root behavior close to the critical voltage is another unsolved puzzle. Fitting the experimental width function shown in Fig. 7, we found that the expression $\Delta\omega \sim (\tilde{V}_0 - \tilde{V}_0^{(\mathrm{cr})})^{1/3}$ fits the width function much better than the expected square root. We do not know how to explain the deviation in the exponent, and, more importantly, whether some physics is contained in it which we have overlooked so far.

VIII. SUMMARY AND CONCLUSIONS

The main thrust of this paper is a detailed analysis and explanation of the excitation mechanism of a collective resonance of uncooled clouds of H_2^+ ions stored in a Paul trap, and driven at about twice the secular frequency ω_z by an additionally applied excitation voltage. We presented ample experimental evidence of the existence of the collective resonance as well as detailed three-dimensional numerical simulations which are able to reproduce qualitatively the essential characteristics of the collective resonance such as location, shape, and width. We also reported some interesting experimental results, such as the bistability of the collective resonance in the vicinity of its low-frequency wing, where the sharp transition to the mother resonance occurs. A simple analytical model extracted from the three-dimensional equations of motion of the stored H_2^+ ions is able to reproduce the results of the three-dimensional computations. Since the simple model retains only the z component of the center-of-mass motion of the ion cloud, the collective resonance is explained as a parametric excitation of the z component of the center-of-mass motion of the ion cloud. This result is backed by experiments which establish that the collective resonance is insensitive to space-charge effects.

Although we are able to explain the most prominent features of the collective resonance, our experiments also leave numerous open questions for future research. The most important among them is the identification of the relevant damping mechanism in our experiments, since this mechanism determines decisively the value and functional behavior of the critical voltage as a function of the number of ions in the cloud. Since the damping constant appears in the expression for the width of the collective resonance, the damping mechanism, indirectly, also determines the width of the col-

lective resonance as a function of the excitation voltage. The most promising direction for future research is an investigation of the nonlinear dynamics of the cloud motion in the vicinity of the $2\omega_r$ resonance, as well as an investigation of the bistability, and possibly multistability, of the cloud in the vicinity of both the $2\omega_r$ and $2\omega_z$ resonances.

ACKNOWLEDGMENTS

We would like to thank E. Teloy for directing our attention to Ref. [11]. The experiment was supported by the Deutsche Forschungsgemeinschaft. X.Z.C. acknowledges a grant from the Deutscher Akademischer Austauschdienst.

[1] W. Paul, W. Osberghaus and E. Fischer, Forsch. Wirtsch. Verkehrsminist. Nordrhein-Westfalen **415**, 1 (1958).
[2] W. Paul, Rev. Mod. Phys. **62**, 531 (1990).
[3] H. Dehmelt, Adv. At. Mol. Phys. **3**, 53 (1967).
[4] R. F. Wuerker, H. Shelton, and R. V. Langmuir, J. Appl. Phys. **30**, 342 (1959).
[5] J. Hoffnagle, R. G. DeVoe, L. Reyna, and R. G. Brewer, Phys. Rev. Lett. **61**, 255 (1988).
[6] R. Blümel, J. M. Chen, E. Peik, W. Quint, W. Schleich, Y. R. Shen and H. Walther, Nature (London) **334**, 309 (1988).
[7] R. Blümel, C. Kappler, W. Quint, and H. Walther, Phys. Rev. A **40**, 808 (1989).
[8] J. Hoffnagle and R. G. Brewer, Phys. Rev. Lett. **71**, 1828 (1993).
[9] J. W. Emmert, M. Moore, and R. Blümel, Phys. Rev. A **48**, 1757 (1993).
[10] M. Moore and R. Blümel, Phys. Rev. A **48**, 3082 (1993).
[11] G. Rettinghaus, Ph. D. thesis, Bonn University, 1965 (unpublished).
[12] K. Jungmann, J. Hoffnagle, R. G. DeVoe, and R. G. Brewer, Phys. Rev. A **36**, 3451 (1987).
[13] F. Vedel and M. Vedel, Phys. Rev. A **41**, 2348 (1990).
[14] F. Vedel, M. Vedel and R. E. March, Int. J. Mass Spectrom. Ion Processes **99**, 125 (1990).
[15] R. Alheit, Ph. D. thesis, Mainz University, 1997.
[16] R. Alheit, M. Hoefer, M. Holzki, G. Werth, and R. Blümel, Verhandlungen DPG **3**, 203 (1997).
[17] J. Guckenheimer and P. Holmes, *Nonlinear Oscillations, Dynamical Systems and Bifurcations of Vector Fields* (Springer, New York, 1983).
[18] A. J. Lichtenberg and M. A. Lieberman, *Regular and Stochastic Motion* (Springer, New York, 1983).
[19] E. Ott, *Chaos in Dynamical Systems* (Cambridge University Press, Cambridge, 1993).
[20] S. Stenholm, Rev. Mod. Phys. **58**, 699 (1986).
[21] R. Alheit, Th. Gudjons, S. Kleineidan, and G. Werth, Rapid Commun. Mass Spectrom. **10**, 583 (1996).
[22] R. Alheit, C. Hennig, R. Morgenstern, F. Vedel, and G. Werth, Appl. Phys. B **61**, 277 (1995).
[23] I. S. Gradshteyn and I. M. Ryzhik, *Table of Integrals, Seris, and Products* (Academic, Boston, 1994).
[24] R. Alheit, X. Z. Chu, M. Hoefer, M. Holzki, G. Werth, and R. Blümel (unpublished).
[25] L. D. Landau and E. M. Lifschitz, *Mechanics* (Pergamon, Oxford, 1960).
[26] H. Schaaf, U. Schmeling, and G. Werth, Appl. Phys. **25**, 249 (1981).